


RESEARCH LETTER

Open Access



# A snapshot of the climate in the Middle Pleistocene inferred from a stalagmite from central Japan

Masataka Sakai<sup>1</sup>, Masako Hori<sup>1\*</sup> , Ryu Uemura<sup>2</sup>, Bassam Ghaleb<sup>3</sup>, Daniele L. Pinti<sup>3</sup>, Mahiro Yumiba<sup>1,4</sup>, Masafumi Murayama<sup>5</sup> and Akihiro Kano<sup>6</sup>

## Abstract

Stalagmites are useful archives in reconstructing paleoclimates: most paleoclimate studies used stalagmites that are distributed in specific locations and ages. We examined a stalagmite (GYM-1) collected from Nara Prefecture, central Japan, where limestone areas are limited. Applying  $^{238}\text{U}$ – $^{234}\text{U}$  method, the ages of GYM-1 were determined as  $744 \pm 70$  to  $677 \pm 74$  ka (based only on analytical uncertainties,  $1\sigma$ ). Even assuming a 10% uncertainty in the initial activity of  $^{234}\text{U}/^{238}\text{U}$ , ( $^{234}\text{U}/^{238}\text{U}$ )<sub>0</sub>, this age could be still older than 460 ka. Temperatures calculated based on  $\delta\text{D}$  in the fluid inclusions and  $\delta^{18}\text{O}$  in the calcium carbonate ranged from 9.0 to 11.9 °C ( $10.8 \pm 0.9$  °C on average) or from 6.0 to 9.1 °C ( $7.9 \pm 0.9$  °C on average) depending on the equation. The estimated temperature suggests that GYM-1 formed during an interglacial period of the Middle Pleistocene. Synchronous behavior of isotopic values with lamination likely reflects seasonal temperature in a highly ventilated cave system.

**Keywords** Stalagmite, Middle Pleistocene, Stable isotopes, Climate record, Uranium disequilibrium method

## Introduction

Stable oxygen isotopic records of stalagmites are useful for reconstructing terrestrial paleoclimates, particularly from the Late Pleistocene to Holocene (e.g., Wang et al. 2001; Genty et al. 2003; Yuan et al. 2004; Dykoski et al. 2005). The thorium-230 ( $^{230}\text{Th}$ ) method provides a

significant advantage for stalagmites by minimizing the dating uncertainty (~1%, Shen et al. 2012; Cheng et al. 2013). However,  $^{230}\text{Th}$  dating is only applicable for specimens formed within the last 650 kyr because the activities of  $^{234}\text{U}$  and  $^{230}\text{Th}$  reach near their equilibrium. The limitation of the dating method results in the restriction of climate records from older stalagmites. Thus, the terrestrial climate in the Early and Middle Pleistocene is rarely supported by stalagmite records.

Stalagmite records in Japan are limited, especially from the mainland (e.g., Shen et al. 2010; Sone et al. 2013; Mori et al. 2018), which are all younger than 100 ka. To approach the geochemical record of the Middle Pleistocene and evaluate isotopic alteration during extended preservation, we applied  $^{238}\text{U}$ – $^{234}\text{U}$  dating to a stalagmite (GYM-1) collected in Nara Prefecture, central Japan. We also analyzed the stable isotopes in calcium carbonate and fluid inclusions in GYM-1 to estimate the paleo-temperature.

\*Correspondence:

Masako Hori

horizon@cc.osaka-kyoiku.ac.jp

<sup>1</sup> Natural Sciences, Osaka Kyoiku University, 4-698-1, Asahigaoka, Kashiwara City, Osaka 582-8582, Japan

<sup>2</sup> Graduate School of Environmental Studies, Nagoya University, Furo-Cho, Chikusa-Ku, Nagoya 464-8601, Japan

<sup>3</sup> GEOTOP, Université du Québec à Montréal, CP 8888 Succ. Centre-Ville H2X 3Y7, Montréal, QC, Canada

<sup>4</sup> Atmosphere and Ocean Research Institute, The University of Tokyo, 5-1-5, Kashiwanoha, Kashiwa City, Chiba 277-8564, Japan

<sup>5</sup> Marine Core Research Institute, Kochi University, 200, Monobe, Nankoku City, Kochi 783-8502, Japan

<sup>6</sup> Graduate School of Science, The University of Tokyo, 7-3-1, Hongo, Bunkyo-Ku, Tokyo 113-0033, Japan

### Sample location

Goyomatsu cave is located in Tenkawa village, central Nara Prefecture, on the Kii Peninsula, Japan (34.26° N, 135.89° E; Fig. 1a,b). The geology of this region belongs to the Chichibu Composite Belt, an accretionary

complex developed from the Carboniferous to the Jurassic. The limestone bearing caves are Permian in age, poor in fossils, and have largely transformed into marble owing to the penetration of Neogene igneous rocks. The modern climate at the Tenkawa Observatory

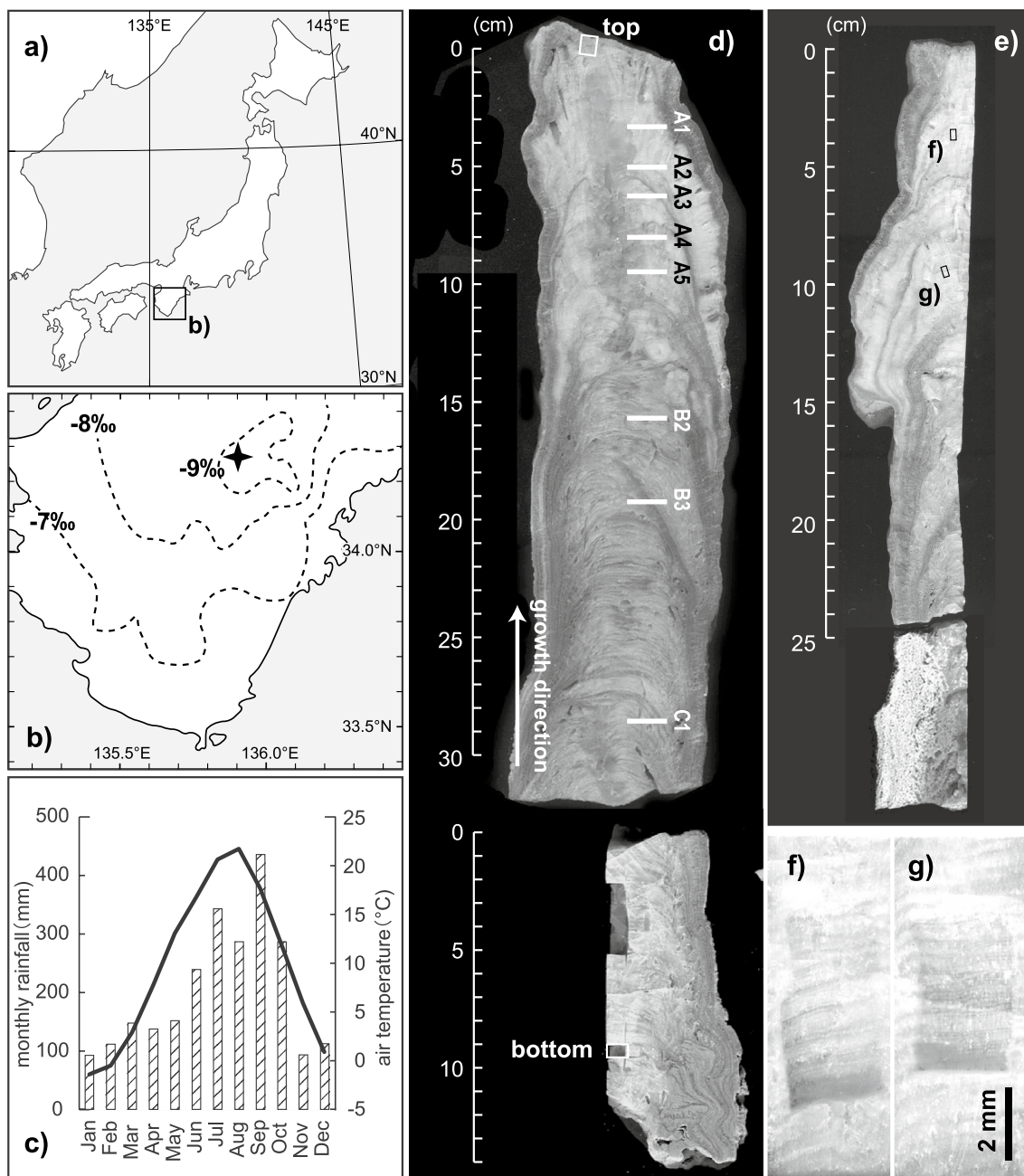


**Fig. 1** **a** Location of Goyomatsu cave on a wide-area map of Japan and **(b)** in the Kii Peninsula. The dashed counter represents the  $\delta^{18}\text{O}$  of rainwater after Ishizuka et al. (2006). **c** The modern monthly air temperature estimated from the record at Gojo Observatory and rainfall amount at Tenkawa Observatory. **d** The cut surface of the stalagmite, GYM-1, used for low-resolution (1 mm) analysis. The horizontal bars with letters and numbers (A1–A5, B2–B3, and C1) represent the positions for the fluid inclusion analyses (see Table S2). White line squares represent the positions for age determination. **e** Another cut surface of GYM-1 showing areas (black line squares) for high-resolution ( $\sim 0.1$  mm) analysis and **f, g** enlarged images

is temperate. Annual precipitation is 2500 mm (average from 1991 to 2020; available at <https://www.data.jma.go.jp/gmd/risk/obsdl/index.php>), where 50% of the annual precipitation occurs from June to September (Fig. 1c). The monthly air temperature at the cave site ranges from  $-1.4$  to  $22$  °C, with an annual average of  $9.8$  °C, based on the altitudinal effect ( $0.6$  °C/100 m) for the observation at Gojo Observatory, located 21 km northwest of Goyomatsu cave.

Goyomatsu cave has two floors with multiple entrances. We collected a 40-cm-long specimen (GYM-1; Fig. 1d–g) approximately 15 m inside from the cave entrance on the lower floor in July 2018. GYM-1 is characterized by a finely laminated structure with light porous and dark transparent layers under reflected illumination (Fig. 1f,g). Dripwater samples were collected from two stalactites a few meters apart from the GYM-1 site. One liter of a dripwater sample was collected from each stalactite for one month in February 2018 when the cave was closed to tourists.

## Methods

### Dating

The stalagmite was cut into halves along the growth direction; the cut surface was polished. The  $^{230}\text{Th}$  and  $^{238}\text{U}$ – $^{234}\text{U}$  dating was performed at GEOTOP, Université du Québec à Montréal. We cut cubic specimens of approximately 1 g each from the top and bottom of the stalagmite (Fig. 1d). Two dripwater samples collected near the stalagmite sites were analyzed to obtain the  $(^{234}\text{U}/^{238}\text{U})_0$  activity ratio. Dripwater samples were filtered through a  $0.22$   $\mu\text{m}$  membrane filter and sealed in PFA bottles. Chemical separation and purification were performed using AG1X8 anion exchange resin (Bio-Rad) and U-Teva resin (Elchrom industry<sup>TM</sup>), following the methods described in Pons-Branchu et al. (2005) and Ghaleb et al. (2019). The isotopic compositions of the purified U and Th fractions were analyzed using a multi-collector inductively coupled plasma mass spectrometer (MC-ICP-MS, Nu II instrument<sup>TM</sup>) at GEOTOP.

Assuming that the dripwater  $^{234}\text{U}/^{238}\text{U}$  activity was the initial  $^{234}\text{U}/^{238}\text{U}$  activity,  $(^{234}\text{U}/^{238}\text{U})_0$ , when the stalagmite was deposited, the ages were calculated as follows:

$$\left( ^{234}\text{U}/^{238}\text{U} \right)_t - 1 = \left\{ \left( ^{234}\text{U}/^{238}\text{U} \right)_0 - 1 \right\} \exp(-\lambda_{234}t), \quad (1)$$

where  $(^{234}\text{U}/^{238}\text{U})_t$  is the current  $^{234}\text{U}/^{238}\text{U}$  activity of the stalagmite and  $\lambda_{234}$  represents the decay constant of  $^{234}\text{U}$  ( $2.8221 \times 10^{-6}$   $\text{yr}^{-1}$ , Cheng et al. 2009; 2013). Dating errors were calculated based on the law of propagation of error, as well as on the uncertainty of  $(^{234}\text{U}/^{238}\text{U})_0$ .

### Stable isotopic analyses

Two different resolutions of the carbonate samples were prepared for oxygen and carbon stable isotopic analyses. For low-resolution analysis, 100  $\mu\text{g}$  of each powdered specimen was collected at 1 mm intervals along the growth axis. The powder specimens were analyzed using a continuous-flow IRMS (MAT Delta Plus, Finnigan) connected to a carbonate pretreatment device, Gas Bench, at the University of Tokyo. Powder carbonate samples were reacted with purified phosphoric acid in a helium-controlled atmosphere at  $60$  °C and maintained for more than 5 h. For high-resolution analysis, 60  $\mu\text{g}$  of each powder specimen was collected at approximately 0.1 mm intervals for clearly laminated positions (Fig. 1e–g) under a high-vision microscope (TGM200XM, Shodensha Inc.). The powder specimens were analyzed using a dual-inlet IRMS (MAT 253, Finnigan) connected to a pretreatment device (Kiel carbonate device, Finnigan) at Kochi University. Samples were reacted with phosphoric acid under vacuum at  $70$  °C. The isotopic ratio was expressed in  $\delta$  notation relative to the Vienna Pee Dee Belemnite (VPDB). The reproducibility of the isotopic ratio was better than  $0.1\%$  for  $\delta^{13}\text{C}$  and  $0.1$ – $0.2\%$  for  $\delta^{18}\text{O}$  ( $1\sigma$ ) on the MAT Delta Plus, whereas it was better than  $0.1\%$  for  $\delta^{13}\text{C}$  and  $0.05\%$  for  $\delta^{18}\text{O}$  ( $1\sigma$ ) on the MAT 253. We also prepared thin sections from the cut specimen at the same positions for the high-resolution analyses.

Ten sections  $16 \times 16$   $\text{mm}^2$  in area and 2 mm in depth were cut from GYM-1 (Fig. 1d) for the isotopic analysis of fluid inclusions. Isotopic values were analyzed using cavity ring-down spectroscopy (CRDS, L2140-i, Picarro Inc.), coupled with an extraction device at Nagoya University, following a continuous standard water background method (de Graaf et al. 2020). Eight sections containing more than 0.2  $\mu\text{L}$  of water were adopted for isotope measurements. The isotopic values of the water samples were expressed relative to the international reference, VSMOW. The reproducibility was better than  $\pm 0.2$  and  $\pm 0.6\%$  for  $\delta^{18}\text{O}$  and  $\delta\text{D}$ , respectively, ( $1\sigma$ ). The  $\delta^{13}\text{C}$  and  $\delta^{18}\text{O}$  in carbonate fraction of the same eight sections were also analyzed by a continuous-flow IRMS (Delta V Advantage, Thermo Fisher Scientific, Inc.) connected to a carbonate pretreatment system (Gas Bench II, Thermo Fisher Scientific, Inc.) at Nagoya University. The isotopic measurements were performed in triplicate, providing standard deviations for the mean ( $1\sigma/\sqrt{n}$ ) better than  $0.1\%$  for both carbon and oxygen. Among the several equations for oxygen isotope fractionation, we adopted two equations: (Coplen 2007; Tremaine et al. 2011).

$$1000 \times \ln \alpha_{\text{CaCO}_3-\text{H}_2\text{O}} = 17.4 \times 1000/(t-273.15) - 28.6 \quad (2)$$

and

$$1000 \times \ln \alpha_{\text{CaCO}_3\text{-H}_2\text{O}} = 16.1 \times 1000 / (t - 273.15) - 24.6 \quad (3)$$

where  $\alpha_{\text{CaCO}_3\text{-H}_2\text{O}}$  represents the oxygen isotopic fractionation factor between water and calcium carbonate.

## Results and discussions

### Timing of stalagmite formation

The two samples collected at the bottom and top of GYM-1 examined for  $^{230}\text{Th}/^{234}\text{U}$  activity ratios exceeding 1 (1.07–1.10, Table S1 and Fig. 2a), likely due to selective uranium loss during diagenetic alteration, such as recrystallization (Lachniet et al. 2012; Bajo et al. 2012). Uranium loss causes serious dating errors for the  $^{230}\text{Th}$  and/or U–Pb method depending on the timing of uranium escape; however, it does not affect the  $^{238}\text{U}$ – $^{234}\text{U}$  method because U dissolution and leaching would not involve  $^{234}\text{U}/^{238}\text{U}$  fractionation. We estimated the initial  $^{234}\text{U}/^{238}\text{U}$  ratio of GYM-1,  $(^{234}\text{U}/^{238}\text{U})_0$ , by measuring the two dripwater samples ( $^{234}\text{U}/^{238}\text{U}$  of  $\sim 1.2$ , Table S1). Applying the mean ratio of the two dripwater samples as  $(^{234}\text{U}/^{238}\text{U})_0$ , the ages of GYM-1 were calculated as  $744 \pm 70$  ka ( $1\sigma$ ) for the bottom and  $677 \pm 74$  ka for the top (Fig. 2b). As a result, the two dates overlapped within mutual errors, making it impossible to obtain further age constraints.

We also considered the uncertainty of  $(^{234}\text{U}/^{238}\text{U})_0$ , which significantly affects the dating error. A previous study on an Italian stalagmite showed the relative standard deviation (RSD) in  $(^{234}\text{U}/^{238}\text{U})_0$  as 4% ( $1\sigma$ ) during 100 kyr (Bajo et al. 2012), while another specimen from the same cave showed a relatively constant  $(^{234}\text{U}/^{238}\text{U})_0$  ratio of 0.5% ( $1\sigma$ ) for the last 16 ka (Bajo et al. 2016). Another study on a travertine deposit (carbonate precipitate from hydrothermal water) showed 10% ( $1\sigma$ ) RSD of  $(^{234}\text{U}/^{238}\text{U})_0$  used for the age construction for the last 300 ka (Ghaleb et al. 2019). Similar range of RSD in  $(^{234}\text{U}/^{238}\text{U})_0$  was also estimated from the stalagmites formed in mainland Japan (1–5%, Shen et al. 2010; Sone et al. 2013; Mori et al. 2018). Applying the largest uncertainty of  $(^{234}\text{U}/^{238}\text{U})_0$  reported in previous studies (10%) to GYM-1, the dating errors were  $\pm 220$  and  $\pm 219$  ka ( $1\sigma$ ) for the top and bottom, respectively. Even in this case, the age of GYM-1 ranged from 456 to 963 ka. This age range does not contradict the  $^{230}\text{Th}/^{234}\text{U}$  activity ratio, which was similar to the secular equilibrium ( $\sim 1$ , Table S1).

### Formation temperature

The low-resolution  $\delta^{18}\text{O}$  values of  $\text{CaCO}_3$  ( $\delta^{18}\text{O}_{\text{cc}}$ ) in GYM-1 ranged from  $-8.2$  to  $-6.4\text{‰}$  with an average of  $-7.3\text{‰}$  (Fig. 3). The  $\delta^{13}\text{C}$  of  $\text{CaCO}_3$  ( $\delta^{13}\text{C}_{\text{cc}}$ ) ranged from  $-9.7$  to  $-5.6\text{‰}$  with an average of  $-7.9\text{‰}$ . Eight pairs of

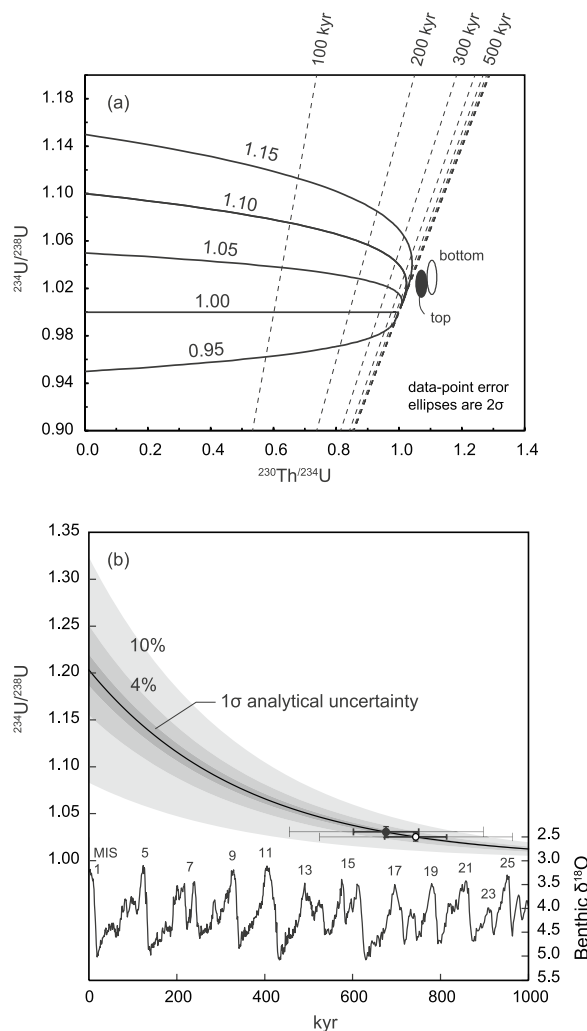


**Fig. 2** a  $^{230}\text{Th}/^{238}\text{U}$  and  $^{234}\text{U}/^{238}\text{U}$  in the classic isotope evolution diagram. b Evolution of the  $^{234}\text{U}/^{238}\text{U}$  activity with a  $^{234}\text{U}/^{238}\text{U}_0$  value of  $1.203 \pm 0.034$  ( $1\sigma$ ). Shaded zone represents uncertainties: the dark shade represents  $1\sigma$  standard deviation calculated from the analytical uncertainties (Table S1); bright shade and the intermediate represent ranges calculated for 10% and 4% deviations in  $(^{234}\text{U}/^{238}\text{U})_0$ , respectively. Thick error bars represent the  $1\sigma$  standard deviation, while thin error bars were estimated from 10% deviations in  $(^{234}\text{U}/^{238}\text{U})_0$ . The last 1000 ka  $\delta^{18}\text{O}$  record of benthic foraminifera (LR04 stack; Lisiecki and Raymo 2005) is also shown. Numbers indicate MIS stages (Railsback et al. 2015)

$\delta^{18}\text{O}$  values from  $\text{CaCO}_3$  and fluid inclusions ( $\delta^{18}\text{O}_{\text{cc}}$  and  $\delta^{18}\text{O}_{\text{fi}}$ , respectively) were applied to the equations from Coplen (2007) and Tremaine et al. (2011). The resulting temperatures ( $T$ ) ranged from 6.5 to 11.3 °C ( $9.3 \pm 1.7$  °C on average) and 3.4 to 8.5 °C ( $6.4 \pm 1.8$  °C on average), respectively.

The analyzed  $\delta D_{\text{fi}}$  and  $\delta^{18}\text{O}_{\text{fi}}$  values yielded a high d-excess (14.3 to 19.9‰; the intercept of the meteoric water line, MWL, Table S2) compared to the

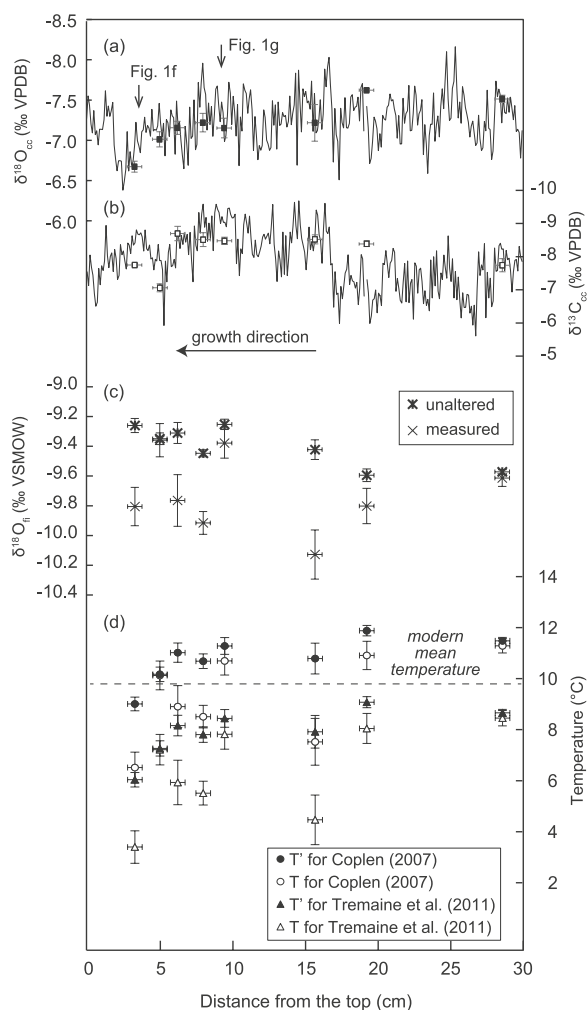


**Fig. 3** Low-resolution records of the (a)  $\delta^{18}\text{O}_{\text{cc}}$  and (b)  $\delta^{13}\text{C}_{\text{cc}}$  values in GYM-1. Squares represent the isotopic values in eight sections. Vertical error bar represents the standard deviation of the mean ( $2\sigma/\sqrt{n}$ ), while horizontal error bar represents  $\pm 5$  mm. c Measured and unaltered  $\delta^{18}\text{O}_{\text{fi}}$  were used to obtain (d) temperatures, T (open symbol) and T' (closed symbol), respectively. Circle and triangle symbols represent temperatures calculated for Coplen (2007) and Tremaine et al. (2011), respectively. Vertical error bar represents  $1\sigma$ , while horizontal error bar represents  $\pm 5$  mm

modern value ( $\sim 14.2\%$ , Ishizuka et al. 2006, Fig. S1). This high d-excess may result from a shift in the local MWL (LMWL) or post-depositional alteration of  $\delta^{18}\text{O}_{\text{fi}}$  (Demény et al. 2016; Uemura et al. 2020). The latter can occur during the isotopic exchange between water and  $\text{CaCO}_3$ , where the amount of oxygen in fluid inclusions is overwhelmed by a large amount of oxygen in the surrounding  $\text{CaCO}_3$ . Such isotopic exchange does not affect the  $\delta D_{\text{fi}}$  values due to the absence of hydrogen in the surrounding matrix. Here, the unaltered  $\delta^{18}\text{O}_{\text{fi}}$  values were estimated from the  $\delta D_{\text{fi}}$  values using the relationship in the modern LMWL ( $\delta D = 8.1 \times \delta^{18}\text{O} + 14.2$ , Ishizuka et al.

2006). Comparing measured  $\delta^{18}\text{O}_{\text{fi}}$  and unaltered  $\delta^{18}\text{O}_{\text{fi}}$ , cut specimens, A2 and C1, showed similar values, while 4 sections, A1, A3, A4, and B2, showed different values (Fig. 3c). This may indicate the heterogeneous alteration of fluid inclusions in GYM-1. The optical image of the stalagmite showed a structural shift at 14 cm from the top: white layer in upper half and relatively compact and translucent layer in bottom half (Fig. 1d), which is not correlate with the difference between measured  $\delta^{18}\text{O}_{\text{fi}}$  and unaltered  $\delta^{18}\text{O}_{\text{fi}}$ . In addition, the LMWL include some uncertainties as seen in modern meteoric waters that show dispersive isotopic values (Fig. S1). Therefore, the precise degree of  $\delta^{18}\text{O}_{\text{fi}}$  alteration and its relationship with the local structure was difficult to be solved. Using unaltered  $\delta^{18}\text{O}_{\text{fi}}$ , the recalculated temperature (T') falls within a narrow range from 9.0 to 11.9 °C ( $10.8 \pm 0.9$  °C on average) for Coplen et al. (2007), and from 6.0 to 9.1 °C ( $7.9 \pm 0.9$  °C on average) for Tremaine et al. (2011) (Fig. 3). According to the results, we considered that T' based on  $\delta D_{\text{fi}}$  and modern LMWL better represents the past temperature. In either case, the post-depositional alteration of  $\delta^{18}\text{O}_{\text{fi}}$  in GYM-1, if present, was not significant because the difference between T and T' was smaller than the difference produced by the equations.

The estimated temperate temperature, similar to the modern climate, suggests GYM-1 likely formed during an interglacial period. Considering the dating error and a 10% uncertainty in  $(^{234}\text{U}/^{238}\text{U})_0$ , potential growth period includes MISs 13, 15, 17, 19, 21, 23, and 25 (Fig. 2).

### High-resolution isotopic record and the effect of ventilation

The high-resolution  $\delta^{18}\text{O}_{\text{cc}}$  analyzed for two selected positions ( $\sim 3.5$  and 9.3 mm from the top; Fig. 1e) in GYM-1 varied from  $-7.8$  to  $-6.6\%$  ( $-7.3\%$  on average) and from  $-8.3$  to  $-7.2\%$  ( $-7.8\%$  on average) with a mean amplitude of 0.4 and 0.6‰, respectively (Fig. 4). A similar pattern was observed in  $\delta^{13}\text{C}_{\text{cc}}$ , which showed a greater amplitude of approximately 2.0‰. The  $\delta^{18}\text{O}_{\text{cc}}$  and  $\delta^{13}\text{C}_{\text{cc}}$  values changed together in a cyclic manner and were significantly correlated with each other ( $R^2 = 0.39$ ). Isotopic changes were roughly coincident with the texture of GYM-1: relatively high values occurred at thick laminae enriched in needle-like pores, whereas low values were at thin and transparent laminae (Fig. 4). Similar features have been reported for fast-growing stalagmites formed in caves affected by ventilation (Mattey et al. 2010; Boch et al. 2011). The cave morphology and the sample proximity to the cave entrance (15 m) supports well-ventilated system. Ventilated conditions raise the growth rate of a stalagmite by accelerating  $\text{CO}_2$  degassing from the dripwater, providing a possibility

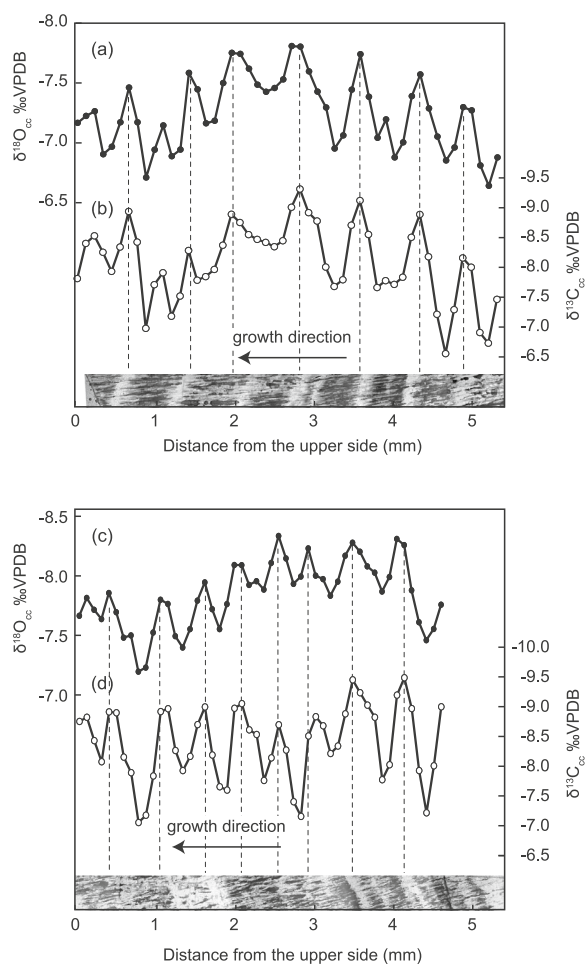


**Fig. 4** High-resolution profiles of  $\delta^{18}\text{O}_{\text{cc}}$  (closed circle) and  $\delta^{13}\text{C}_{\text{cc}}$  values (open circle) at two positions revealing lamination. The sampling position of (a) and (b) refers to Fig. 1f, while the position of (c) and (d) refers to Fig. 1g. Transmitted images of the thin sections are also shown

of extracting seasonal temperatures. According to the linear relationship between  $T'$  and  $\delta^{18}\text{O}_{\text{cc}}$  (Fig. S2), temperature can be roughly estimated from  $\delta^{18}\text{O}_{\text{cc}}$ . In this case, the high-resolution  $\delta^{18}\text{O}_{\text{cc}}$  correspond to temperatures from 9.0 to 14.0 °C or from 6.3 to 11.4 °C, depending on the equation, with a relatively constant amplitude of 2–3 °C. This range is reasonable for the cave air temperature. Although dry air fed by ventilation can raise oxygen isotopic fractionation due to evaporation, this effect is minimized when drip rate is sufficiently high (Rampelbergh et al. 2014; Feng et al. 2014). The synchronous change in  $\delta^{18}\text{O}_{\text{cc}}$  and  $\delta^{13}\text{C}_{\text{cc}}$  in GYM-1 primarily reflects the annual changes in temperature and partial pressure of  $\text{CO}_2$  in the cave air, which tend to be high in summer and low in winter.

## Conclusions

Stalagmites older than 650 ka are challenging owing to the increasing risks of alteration, in addition to the difficulties in applying  $^{230}\text{Th}$  dating methods. We analyzed a well-laminated stalagmite (GYM-1) collected at Goyomatsu Cave, Nara Prefecture, central Japan. Two ages for the top and bottom of the stalagmite were determined by  $^{238}\text{U}$ – $^{234}\text{U}$  methods as  $744 \pm 70$  and  $677 \pm 74$  ka, respectively (where errors are based only on analytical uncertainties,  $1\sigma$ ). Even when accounting for a 10% uncertainty in  $(^{234}\text{U}/^{238}\text{U})_0$ , GYM-1 could be older than 460 ka, indicating that GYM-1 is concurrently the oldest among dated stalagmites in Japan. In this study, we could only obtain two ages to estimate the timing of GYM-1 formation. Further U-series analyses on multiple portions from the stalagmite would help evaluate the U-loss during the preservation and the initial  $^{234}\text{U}/^{238}\text{U}$  variations during the growth period. The temperature estimated from  $\delta^{18}\text{O}_{\text{cc}}$  and  $\delta D_{\text{fi}}$  ranged from 9.0 to 11.9 °C or from 6.0 to 9.1 °C, similar to the modern climate. The high-resolution isotopic analysis of GYM-1 showed synchronous behavior of the  $\delta^{18}\text{O}_{\text{cc}}$  and  $\delta^{13}\text{C}_{\text{cc}}$  values with the lamination, suggesting that GYM-1 formed in a ventilated system. If the isotopic equilibrium can be established, GYM-1 is a potential stalagmite recording the seasonal temperature in the interglacial stages of the Middle Pleistocene.

## Abbreviations

IRMS Isotopic ratio mass spectrometer  
MIS Marine isotope stage

## Supplementary Information

The online version contains supplementary material available at <https://doi.org/10.1186/s40562-024-00357-3>.

Supplementary Material 1.

## Acknowledgements

Sampling was performed under the permission of the Educational Board of Nara Prefecture and monitored in the presence of the Administration of Dorokawa. The fluid inclusion analysis was assisted by Kyoko Osawa, Nagoya University. High-resolution analysis with ~0.1 mm resolution was performed under the cooperative research program of the Center for Advanced Marine Core Research (CMCR) at Kochi University (No. 22A044 and 22B040 to MH).

## Author contributions

MS conducted fieldwork and analyzed the low-resolution stable isotope data. MH conceptualized the study, analyzed the data, and wrote the manuscript. RU conducted fluid inclusion analysis and contributed to interpretation. BG and DLP conducted dating. MY analyzed the high-resolution stable isotope data. MM and AK contributed to the stable isotopic analysis of  $\text{CaCO}_3$ . All authors read and approved the final manuscript.

## Funding

This study was supported by the Japan Society for the Promotion of Science (16H02235 and 20H00191 to AK and 20H00628 to RU).

**Availability of data and materials**

The datasets generated and/or analyzed in this study are available from the corresponding author on reasonable request.

**Declarations****Competing interests**

The authors declare no conflicts of interest.

Received: 16 January 2024 Accepted: 16 August 2024

Published online: 09 September 2024

**References**

- Bajo P, Drysdale R, Woodhead J, Hellstrom J, Zanchetta G (2012) High-resolution U-Pb dating of an early Pleistocene stalagmite from Corchia cave (central Italy). *Quaternary Geochronol* 14:5–17
- Bajo P, Hellstrom J, Frisia S, Drysdale R, Black J, Woodhead J, Borsato A, Zanchetta G, Wallace MW, Regattieri E, Haese R (2016) "Cryptic" diagenesis and its implications for speleothem geochronologies. *Quat Sci Rev* 140:17–28
- Boch R, Spötl C, Frisia S (2011) Origin and palaeoenvironmental significance of lamination in stalagmites from Katerloch cave, Austria. *Sedimentology* 58:508–531
- Cheng H, Edwards RL, Broecker WS, Denton GH, Kong X, Wang Y, Zhang R, Wang X (2009) Ice age terminations. *Science* 326:248–252
- Cheng H, Edwards RL, Shen CC, Polyak VJ, Asmerom Y, Woodhead J, Hellstrom J, Wang Y, Kong X, Spötl C, Wang X, Alexander EC Jr (2013) Improvements in  $^{230}\text{Th}$  dating,  $^{230}\text{Th}$  and  $^{234}\text{U}$  half-life values, and U-Th isotopic measurements by multi-collector inductively coupled plasma mass spectrometry. *Earth Planet Sci Lett* 371–372:82–91
- Coplen TB (2007) Calibration of the calcite-water oxygen-isotope geothermometer at Devils Hole, Nevada, a natural laboratory. *Geochim Cosmochim Acta* 71:3948–3957
- de Graaf S, Vonhof HB, Weissbach T, Wassenburg JA, Levy EJ, Kluge T, Haug GH (2020) A comparison of isotope ratio mass spectrometry and cavity ring-down spectroscopy techniques for isotope analysis of fluid inclusion water. *Rapid Commun Mass Spectrom*. <https://doi.org/10.1002/rcm.883>
- Demény A, Czuppon G, Kern Z, Leél-Óssy S, Németh A, Szabó M, Tóth M, Wu CC, Shen CC, Molnár M, Németh T, Németh P, Óvári M (2016) Recrystallization-induced oxygen isotope changes in inclusion-hosted water of speleothems—paleoclimatological implications. *Quat Int* 415:25–32
- Dykoski CA, Edwards RL, Cheng H, Yuan D, Cai Y, Zhang M, Lin Y, Qing J, An Z, Revenaugh J (2005) A high-resolution, absolute-dated Holocene and deglacial Asian monsoon record from Dongge cave, China. *Earth Planet Sci Lett* 233:71–86
- Feng W, Casteel RC, Banner JL, Heinze-Fry A (2014) Oxygen isotope variations in rainfall, drip-water and speleothem calcite from a well-ventilated cave in Texas, USA: assessing a new speleothem temperature proxy. *Geochim Cosmochim Acta* 127:233–250
- Genty D, Blamart D, Ouahdi R, Gilmour M, Baker A, Jouzel J, Van-Exter S (2003) Precise dating of Dansgaard-Oeschger climate oscillations in western Europe from stalagmite data. *Nature* 421:833–837
- Ghaleb B, Falgueres C, Carluot J, Pozzi JP, Mahieux G, Boudad L, Rousseau L (2019) Timing of the Brunhes-Matuyama transition constrained by U-series disequilibrium. *Sci Rep* 9:6039. <https://doi.org/10.1038/s41598-019-42567-2>
- Ishizuka M, Sone Y, Li H, Hirata T (2006) Effect of enriched early dropped rainwater on mesoscale isotopic distribution in surface water on the Kii peninsula Japan. *Water Res*. <https://doi.org/10.1029/2004WR003810>
- Lachniet MS, Bernal JP, Asmerom Y, Polyak V (2012) Uranium loss and aragonite-calcite age discordance in a calcitized aragonite stalagmite. *Quat Geochronol* 14:26–37
- Lisiecki LE, Raymo ME (2005) A Pliocene-Pleistocene stack of 57 globally distributed benthic  $\delta^{18}\text{O}$  records. *Paleoceanography*. <https://doi.org/10.1029/2004PA001071>
- Mattey DP, Fairchild IJ, Atkinson TC, Latin JP, Ainsworth M, Durrell R (2010) Seasonal microclimate control of calcite fabrics, stable isotopes and trace elements in modern speleothem from St Michaels cave, Gibraltar. *Geol Soc Spec Publ* 336:323–344
- Mori T, Kashiwagi K, Amekawa S, Kato H, Okumura T, Takashima C, Wu CC, Shen CC, Quade J, Kano A (2018) Temperature and seawater isotopic controls on two stalagmite records since 83 ka from maritime Japan. *Quat Sci Rev* 192:47–58
- Pons-Branchu E, Hillaire-Marcel C, Deschamps P, Ghaleb B, Sinclair DJ (2005) Early diagenesis impact on precise U-series dating of deep-sea corals: example of a 100–200 years old *Lophelia pertusa* sample from the north-east Atlantic. *Geochim Cosmochim Acta* 69:4865–4879
- Railsback LB, Gibbard PL, Head MJ, Voarintsoa NRG, Toucanne S (2015) An optimized scheme of lettered marine isotope substages for the last 1.0 million years, and the climatostratigraphic nature of isotope stages and substages. *Quat Sci Rev* 111:94–106
- Rampelbergh MV, Verheyden S, Allan M, Quinif Y, Keppens E, Claeys P (2014) Monitoring of a fast-growing speleothem site from the Han-sur-Lesse cave, Belgium, indicates equilibrium deposition of the seasonal  $\delta^{18}\text{O}$  and  $\delta^{13}\text{C}$  signals in the calcite. *Clim past* 10:1871–1885
- Shen C-C, Kano A, Hori M, Lin K, Chiu T-C, Burr GS (2010) East Asian monsoon evolution and reconciliation of climate isotope records from Japan and Greenland during the last deglaciation. *Quat Sci Rev* 29:3327–3335
- Shen CC, Wu CC, Cheng H, Edwards RL, Hsieh YT, Gallet S, Chang CC, Li TY, Lam DD, Kano A, Hori M, Spötl C (2012) High-precision and high-resolution carbonate  $^{230}\text{Th}$  dating by Mc-ICP-MS with SEM protocols. *Geochim Cosmochim Acta* 99:71–86
- Sone T, Kano A, Okumura T, Kashiwagi K, Hori M, Jiang X, Shen C-C (2013) Holocene stalagmite oxygen isotopic record from the Japan sea side of the Japanese islands, as a new proxy of the east Asian winter monsoon. *Quat Sci Rev* 75:150–160
- Tremaine DM, Froelich PN, Wang Y (2011) Speleothem calcite farmed in situ: modern calibration of  $\delta^{18}\text{O}$  and  $\delta^{13}\text{C}$  paleoclimate proxies in a continuously-monitored natural cave system. *Geochim Cosmochim Acta* 75:4929–4950
- Uemura R, Kina Y, Shen CC, Omime K (2020) Experimental evaluation of oxygen isotopic exchange between inclusion water and host calcite in speleothems. *Clim past* 16:17–27
- Wang YJ, Cheng H, Edwards RL, An ZS, Wu JY, Shen C-C, Dorale JA (2001) A high-resolution absolute-dated late Pleistocene monsoon record from Hulu cave, China. *Science* 294:2345–2348
- Yuan D, Cheng H, Edwards RL, Dykoski CA, Kelly MJ, Zhang M, Qing J, Lin Y, Wang Y, Wu J, Dorale JA, An Z, Cai Y (2004) Timing, duration, and transitions of the last interglacial Asian monsoon. *Science* 304:575–578

**Publisher's Note**

Springer Nature remains neutral with regard to jurisdictional claims in published maps and institutional affiliations.